
Efficient Probabilistic Performance Bounds for Inverse Reinforcement Learning

Daniel S. Brown

Department of Computer Science
University of Texas at Austin
dsbrown@cs.utexas.edu

Scott Niekum

Department of Computer Science
University of Texas at Austin
sniekum@cs.utexas.edu

Abstract

In the field of reinforcement learning there has been recent progress towards safety and high-confidence bounds on policy performance. However, to our knowledge, no methods exist for determining high-confidence safety bounds for a given evaluation policy in the inverse reinforcement learning setting—where the true reward function is unknown and only samples of expert behavior are given. We propose a method based on Bayesian Inverse Reinforcement Learning that uses demonstrations to determine practical high-confidence bounds on the difference in expected return between any evaluation policy and the expert’s underlying policy. A sampling-based approach is used to obtain probabilistic confidence bounds using the financial Value at Risk metric. We empirically evaluate our proposed bound on a standard navigation task for a wide variety of ground truth reward functions. Empirical results demonstrate that our proposed bound provides significant improvements over a standard feature count-based approach: providing accurate, tight bounds even for small numbers of noisy demonstrations.

1 Introduction

There is a growing interest in safety and risk-sensitive metrics for machine learning and artificial intelligence systems, especially for systems that interact with their environment [8]. In the field of finance, it is common to base investment decisions on risk measures such as Value at Risk or Conditional Value at Risk [12], that take into account uncertainty. Recently these financial risk measures as well as other risk-centric approaches have been applied to planning in Markov Decision Processes [6] and reinforcement learning [18, 8]; however, to the best of our knowledge, no one has investigated how to obtain sample-efficient, risk-aware safety bounds on the performance of a policy under an unknown reward function, as is the case when learning from demonstrations [2]. In this work we propose a general method for obtaining high-confidence safety bounds on the policy return difference Value at Risk [12] (the α -quantile worst-case performance) between any evaluation policy and the optimal policy under the demonstrator’s unobserved reward function.

Learning from demonstration (LfD) is a popular method to learn a skill or policy by simply observing demonstrations from an expert [2]. One popular variant of LfD is Inverse Reinforcement Learning (IRL) [15] where the goal is to infer the reward function that resulted in the demonstrations. LfD techniques based on IRL have potential applications in many settings such as manufacturing, home and hospital care, and autonomous driving. In these types of real-world settings it is important, and perhaps critical, to provide safety bounds on a learned policy. While there are many definitions of safety, we focus on bounding the expected difference in return between a given evaluation policy and the optimal policy under the expert’s reward, when both are evaluated on the demonstrator’s reward function. For example, consider a hospital assistant robot that has learned from demonstrations how to lift a patient out of bed. Before deploying this learned policy, we want to guarantee with high-confidence that the robot’s learned policy performs within some allowable error of the optimal

policy under the expert’s reward. An expert may want to continue to give demonstrations until the robot’s confidence about its performance with respect to the demonstrator is above some safety level.

In this work we assume that there is an unobserved ground truth reward function that the expert attempts (perhaps unsuccessfully) to maximize. If we were able to obtain the demonstrator’s true reward function, we could recover the optimal policy using dynamic programming or reinforcement learning. However, the problem of Inverse Reinforcement Learning is ill-posed—there are an infinite number of reward functions that result in the same optimal behavior. Thus, rather than trying to find a single reward function that explains the demonstrations we seek a risk-sensitive bound on performance that takes into account the entire distribution of likely reward functions. To obtain this bound we use the α -Value-at-Risk (α -VaR) [12], the α -quantile worst outcome, of the difference in expected return between an evaluation policy and the optimal policy under the expert’s true reward, when both policies are evaluated on the demonstrator’s unknown reward function.

Our method uses a Markov-Chain-Monte Carlo sampling method based on Bayesian Inverse Reinforcement Learning [17] to sample likely reward functions given the demonstrations. Using samples of likely reward functions from the posterior, we compute samples of the expected value difference between the unknown optimal policy under the expert’s unknown reward function and the given evaluation policy. These samples are then used to calculate a $(1 - \delta)$ probabilistic upper bound on the α -VaR. We obtain this bound without knowing the expert’s policy or true reward function.

Our main contributions are summarized as follows: (1) We formalize the problem of high-confidence policy evaluation in the inverse reinforcement learning domain; (2) We present the first general method for obtaining high-confidence bounds on the performance difference between any evaluation policy and the optimal policy for a demonstrator’s true unknown reward; (3) We empirically evaluate our proposed Value at Risk bound on a standard navigation task and demonstrate that our proposed bound is a significant improvement over a baseline based on feature counts, and that it provides accurate, tight bounds even for small numbers of noisy demonstrations.

2 Preliminaries

2.1 Markov decision processes

A Markov decision process (MDP) is defined as a tuple $\langle S, A, T, R, \gamma, p_0 \rangle$ where S is the set of states, A is the set of actions, $T : S \times A \times S \rightarrow [0, 1]$ is the transition function, $R : S \rightarrow \mathbb{R}$ is the reward function, $\gamma \in [0, 1)$ is the discount factor, and p_0 is the initial state distribution.

A policy π is a mapping from states to a probability distribution over actions. The value of a policy π under reward function R is denoted as $V^\pi(R) = \mathbb{E}_{s_0 \sim p_0} [\sum_{t=0}^{\infty} \gamma^t R(s_t) | \pi]$. The value of executing policy π starting at state $s \in S$ is recursively defined as $V^\pi(s, R) = R(s) + \gamma \sum_{a \sim \pi(s)} \sum_{s' \in S} T(s, a, s') V^\pi(s', R)$ and the value of policy π can be written as $V^\pi(R) = \sum_{s \in S} p_0(s) V^\pi(s, R)$. Given a reward function R , the Q-value of a state-action pair (s, a) is defined as $Q^\pi(s, a, R) = R(s) + \gamma \sum_{s' \in S} T(s, a, s') V^\pi(s', R)$. We denote the optimal value and Q-value functions as $V^*(R) = \max_{\pi} V^\pi(R)$ and $Q^*(s, a, R) = \max_{\pi} Q^\pi(s, a, R)$, respectively.

As is common in the literature [1, 23], we assume that the reward function can be expressed as a linear combination of features, so that $R(s) = w^T \phi(s)$ where $w \in \mathbb{R}^k$ is the k -dimensional feature weights. Thus, we can write the value of a policy as $V^\pi(R) = \mathbb{E}[\sum_{t=0}^{\infty} \gamma^t w^T \phi(s_t) | \pi] = w^T \mu(\pi)$, where $\mu(\pi) = \mathbb{E}[\sum_{t=0}^{\infty} \gamma^t \phi(s_t) | \pi]$ are the expected feature counts. Note that this does not typically affect the expressiveness of the reward function since ϕ can be a non-linear function. Given ϕ , the reward function is fully specified by the feature weights w . Thus, we refer to the feature weights w and the reward function R interchangeably.

2.2 Bayesian inverse reinforcement learning

In IRL we are given an MDP without a reward function, denoted $\text{MDP} \setminus R$. Given a set of demonstrations, $D = \{(s_1, a_1), \dots, (s_m, a_m)\}$, consisting of state-action pairs, the IRL problem is to recover the reward function R^* of the demonstrator. Because this problem is ill-posed, IRL algorithms use a variety of heuristics and simplifying assumptions to find an estimate of R^* [7].

Bayesian IRL (BIRL) [17] seeks to estimate the posterior over reward functions given demonstrations, $P(R|D) \propto P(D|R)P(R)$. BIRL makes the assumption that actions in states with higher Q-values are exponentially more likely to be chosen, resulting in the likelihood function

$$P(D|R) = \prod_i P((s_i, a_i)|R) = \prod_{(s,a) \in D} \frac{e^{cQ^*(s,a,R)}}{\sum_{b \in A} e^{cQ^*(s,b,R)}} \quad (1)$$

where $Q^*(s, a, R)$ is the optimal Q-value function for reward R and c is a parameter representing the confidence in the demonstrator’s optimality. Equation 1 gives greater likelihood to rewards for which the action taken by the expert, a , has a higher Q-value than the other alternative actions.

Samples from the posterior $P(R|D)$ are obtained through Markov Chain Monte Carlo (MCMC) sampling. Feature weights are sampled according to a proposal distribution and for each sample the MDP is solved to obtain the sample’s likelihood and determine the transition probabilities within the Markov chain. An estimate of the expert’s reward function can be found by averaging the feature weights in the resulting chain to obtain the mean reward function [17] or by using the maximum a posteriori (MAP) estimate [5]. Some of the advantages of BIRL, compared to many other IRL algorithms are (1) it finds a distribution over likely rewards, (2) the state-action pairs in D can be partial demonstrations or even non-contiguous state action pairs, and (3) it explicitly models the sub-optimality of the demonstrator.

3 Problem definition

We assume that we are given an MDP \mathcal{R} and samples $D = \{(s_1, a_1), \dots, (s_m, a_m)\} | (s_i, a_i) \sim \pi_{\text{demo}}\}$ of state-action pairs from a demonstrator’s policy π_{demo} . We make the common assumption [1, 17] that the demonstrator attempts to maximize total return under the reward R^* by executing a possibly sub-optimal, stationary policy π_{demo} .

Given any evaluation policy π_{eval} , our goal is to find an upper bound on the *Expected Value Difference* (EVD) [5] of π_{eval} under the unknown reward R^* , defined as

$$\text{EVD}(\pi_{\text{eval}}, R^*) = V^*(R^*) - V^{\pi_{\text{eval}}}(R^*) \quad (2)$$

where $V^\pi(R) = \mathbb{E}_{s_0 \sim p_0} [\sum_{t=0}^{\infty} \gamma^t R(s_t) | \pi]$ and $V^*(R) = \max_{\pi} \mathbb{E}_{s_0 \sim p_0} [\sum_{t=0}^{\infty} \gamma^t R(s_t) | \pi]$. Thus, we seek to bound the difference in expected return between the evaluation policy π_{eval} and π^* , the policy that is optimal with respect to the demonstrator’s unknown reward R^* .

Because IRL is ill-posed there is an infinite family of rewards that can induce the optimal policy π^* . Because an optimal policy is invariant to any non-negative scaling of the reward function, bounding EVD is also ill-posed, as we can multiply the feature weights w by any $c > 0$ to scale EVD to be anywhere in the range $[0, \infty)$. To avoid this scaling issue we assume that $\|w\|_1 = 1$. Note, that this assumption only eliminates the trivial all-zero reward function as all other reward functions can be appropriately normalized. While setting $\|w\|_1$ eliminates the scaling problem, there can still be infinitely many rewards that induce any optimal policy. Thus we formalize our problem as follows:

High-confidence policy evaluation for IRL Given an MDP \mathcal{R} , an evaluation policy π_{eval} , and a set of demonstrations D , find a $(1 - \delta)$ confidence bound on $\text{EVD}(\pi_{\text{eval}}, R^*)$, where $R^* = w^{*T} \phi(s)$ is the demonstrator’s unobserved reward function.

4 Worst-case feature count bound

Before we give the full details of our approach, we first derive a simple worst-case bound based on feature counts that we use as a baseline. This baseline is a direct extension of the the idea of using expected feature counts [1] to bound the expected value difference of any evaluation policy. As a reminder, we use the notation $\mu(\pi) = \mathbb{E}[\sum_{t=0}^{\infty} \gamma^t \phi(s_t) | \pi]$ to represent the expected feature counts of policy π .

Given any evaluation policy π_{eval} , Abbeel and Ng [1] showed that if we assume $\phi(s) : S \rightarrow [0, 1]^k$, $\|w\|_1 \leq 1$, and know the demonstrator’s expected feature counts $\mu^* = \mu(\pi_{\text{demo}})$, then $\|\mu^* - \mu(\pi_{\text{eval}})\|_2 \leq \epsilon$ implies that $V^{\pi_{\text{demo}}}(R) - V^{\pi_{\text{eval}}}(R) = w^T(\mu^* - \mu(\pi_{\text{eval}})) \leq \epsilon$ for any reward

function $R(s) = w^T \phi(s)$. If π_{demo} is optimal, then $w^T(\mu^* - \mu(\pi_{\text{eval}})) = \text{EVD}(\pi_{\text{eval}}, R^*) \leq \epsilon$ so $\|\mu^* - \mu(\pi_{\text{eval}})\|_2$ gives an upper bound on $\text{EVD}(\pi_{\text{eval}}, R^*)$. Furthermore, the worst-case feature count bound is the objective value of the following maximization problem

$$\max_w \quad w^T(\mu^* - \mu(\pi_{\text{eval}})) \quad (3)$$

$$\text{subject to} \quad \|w\|_1 = 1. \quad (4)$$

This is simply an optimal resource allocation problem and the solution is to put all of our budget for w on the feature with maximal feature count difference, giving the solution $\|\mu^* - \mu(\pi_{\text{eval}})\|_\infty$.

Note that in practice we do not know μ^* , but we can use demonstrated trajectories to estimate of the demonstrator’s expected feature counts as

$$\hat{\mu}^* = \frac{1}{|D|} \sum_{i=1}^{|D|} \sum_{t=0}^{\infty} \gamma^t \phi(s_t^{(i)}), \quad (5)$$

where i indexes over the trajectories and t over the state sequence contained in each demonstrated trajectory. Thus, the empirical *worst-case feature count bound* can be stated as

$$\text{WFCB}(\pi_{\text{eval}}, D) = \|\hat{\mu}^* - \mu(\pi_{\text{eval}})\|_\infty. \quad (6)$$

Note that for this bound to be a guaranteed upper bound on $\text{EVD}(\pi_{\text{eval}}, R^*)$, π_{demo} must be optimal and the empirical estimate of the expert’s feature counts $\hat{\mu}^*$ needs to converge to μ^* , which theoretically requires a large number of demonstrations [1]. Other important limitations of this bound are that it requires complete trajectories to accurately calculate expected feature counts and it does not explicitly use information about the transition dynamics of the problem or what actions were taken by the expert in which states.

5 Bounding Value at Risk

The worst-case feature count bound described in the previous section only requires sampled trajectories from the expert, but completely ignores the structure of the problem—giving a worst-case bound that will likely be overly pessimistic. Our approach is to obtain a probabilistic worst-case bound that uses the structure of the problem (transition dynamics and actions taken by the expert in each state) to find bound on EVD using rewards that are most likely given the demonstrations.

We propose a probabilistic confidence bound on the α -Value at Risk for $\text{EVD}(\pi_{\text{eval}}, R^*)$. Given an MDP \mathcal{R} and a set of state-action pairs $D = \{(s_1, a_1), \dots, (s_m, a_m)\}$, we wish to estimate the Value at Risk of an evaluation policy π_{eval} . We use the notation of Tamar et al. [18] and formally define the α -Value-at-Risk of a random variable Z as

$$\nu_\alpha(Z) = F_Z^{-1}(\alpha) = \inf\{z : F_Z(z) \geq \alpha\} \quad (7)$$

where $\alpha \in (0, 1)$ is the quantile level and $F_Z(z) = Pr(Z \leq z)$ is the cumulative distribution function of random variable Z .

To bound $\text{EVD}(\pi_{\text{eval}}, R^*)$ we use samples from the posterior $P(R|D)$. Thus, we seek to calculate $\nu_\alpha(Z)$ where $Z = \text{EVD}(\pi_{\text{eval}}, R)$ for $R \sim P(R|D)$. We note that using the EVD rather than a standard feature count bound, as discussed in the previous section, is desirable for two main reasons. The first reason is that it works well with partial, noisy demonstrations. This is because EVD compares the evaluation policy against the optimal policy for reward R , not the actual states visited by the potentially sub-optimal demonstrator. Second, the EVD explicitly takes into account the full initial state distribution. Thus, EVD measures the generalizability error of an evaluation policy by evaluating the expected return over all states with support under p_0 , even if demonstrations have only been sampled from a small number of possible initial states.

As motivated in Section 3, we assume $\|w\|_1 = 1$. Thus, to find $P(R|D)$ we use a modified version of the BIRL Policy Walk Algorithm [17] that ensures that our proposal samples of w during MCMC stay on the L1-norm unit ball. Details can be found in Appendix A. Using MCMC, we generate a sequence of sampled rewards $\mathcal{R} = \{R : R \sim P(R|D)\}$ from the posterior distribution over true reward functions given the demonstrations. For each sample $R_i \in \mathcal{R}$ we then calculate

$$Z_i = \text{EVD}(\pi_{\text{eval}}, R_i) = V^*(R_i) - V^{\pi_{\text{eval}}}(R_i) \quad (8)$$

Algorithm 1 $(1 - \delta)$ Confidence Bound on the α -Value-at-Risk

```
1: input: MDP\mathcal{R}, \pi_{\text{eval}}, D, \alpha, \delta
2: \mathcal{R} \leftarrow \text{BIRL}(\text{MDP}\backslash\mathcal{R}, D) \quad \triangleright \text{sample from posterior using L1-unit norm walk}
3: for R_i \in \mathcal{R} do
4:   Z_i = V^*(R_i) - V^{\pi_{\text{eval}}}(R_i) \quad \triangleright \text{compute sample EVD}
5: Y = \text{sort}(Z) \quad \triangleright \text{sort into ascending order statistics}
6: k = \lceil N\alpha + F_{\mathcal{N}}^{-1}(1 - \delta)\sqrt{N\alpha(1 - \alpha)} - \frac{1}{2} \rceil \quad \triangleright \text{index of } (1 - \delta) \text{ confidence bound on } \alpha\text{-VaR}
7: return Y_k
```

giving us a sample from the posterior distribution over expected value differences.

To obtain a point estimate of α -VaR we can sort the resulting samples of Z in ascending order to obtain the order statistics Y , and then take the α -quantile. However, this does not take into account the number of samples or our confidence in this point estimate. Instead of using a point estimate, we compute a single-sided $(1 - \delta)$ confidence bound on the α -VaR. Given a sample Z_i , we have that $P(Z_i < \nu_\alpha(Z)) = \alpha$. Thus, for any order statistic Y_j , we can use the normal approximation of the binomial distribution to obtain

$$P(\nu_\alpha(Z) \leq Y_j) = \sum_{i=1}^j \binom{N}{i} \alpha^i (1 - \alpha)^{N-i} \approx F_{\mathcal{N}}\left(j + \frac{1}{2} \mid N\alpha, N\alpha(1 - \alpha)\right). \quad (9)$$

where F_Z is the CDF of the normal distribution with $\mu = N\alpha$ and $\sigma^2 = N\alpha(1 - \alpha)$ and $1/2$ is added to the index j as a continuity correction [11]. To obtain the index k of the order statistic such that $P(\nu_\alpha(Z) \leq Y_k) \geq (1 - \delta)$ we invert Equation 9 using the inverse of the standard normal CDF, $F_{\mathcal{N}}^{-1}$ to get $k = \lceil N\alpha + F_{\mathcal{N}}^{-1}(1 - \delta)\sqrt{N\alpha(1 - \alpha)} - \frac{1}{2} \rceil$. Our full approach is summarized in Algorithm 1.

The main advantages of our approach are as follows: (1) our proposed bound takes full advantage of all of the information contained in the transition dynamics and demonstrations, (2) it does not require optimal demonstrations, (4) it inherits from BIRL the ability to work with partial demonstrations, even disjoint state-action pairs, and (5) it allows for domain knowledge in the form of a prior.

6 Empirical results

For an upper bound on the expected value difference to be useful, it needs to meet several criteria: (1) the upper bound should be accurate with high-confidence (rarely underestimating the true expected value difference), (2) the bound should be tight with respect to the true expected value difference, and (3) the previous two criteria should be true even when given a small number of demonstrations. We use a standard grid world navigation benchmark [1, 17, 5] to validate that our proposed VaR Bound satisfies these criteria. We compare our high-confidence α -VaR bound with the worst-case feature count bound (WFCB) defined in Equation 6. All results for α -VaR bounds are reported as 95% confidence bounds ($\delta = 0.05$). We examine the affects of both optimal and sub-optimal demonstrations, as well as the sensitivity of our approach to the confidence parameter c and choice of evaluation policy, π_{eval} . Implementation specific details are given in Appendix B.

6.1 Grid world navigation task

We empirically evaluate our approach on a standard navigation task on an $N \times N$ grid world. The actions are up, down, left and right. Transitions are noisy with an 70% chance of moving in the desired direction and 30% chance of going in one of the directions perpendicular to the chosen direction. Each state s has a feature vector $\phi(s)$ of length F associated with it that determines the terrain type. The cost of traveling on different terrains is unknown and must be inferred from demonstrations. To show that our results are not an artifact of a specific reward function or specific feature structure, we evaluate the performance bounds over many random grid worlds each with a randomly chosen ground truth reward. We use a 9x9 grid world navigation task with 8 one-hot binary features. We assume an initial state distribution p_0 that is uniform over 9 different states spread across the grid. When generating M demonstrations we select M states in the support of p_0 , without replacement, and give a rollout from each selected initial state. When measuring accuracy and bound errors, we compare with the true expected value difference over the full initial state distribution.

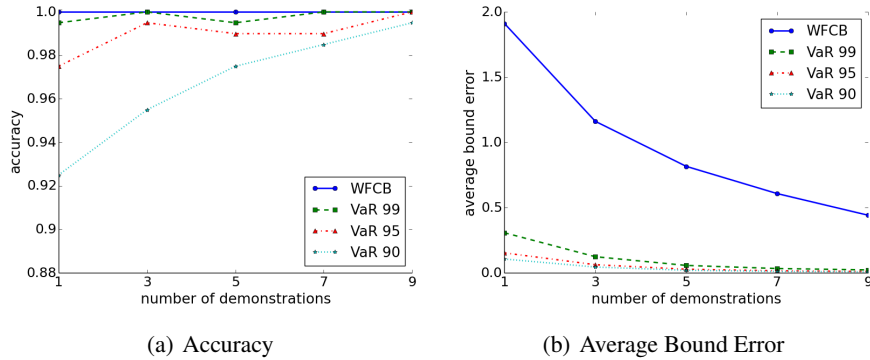


Figure 1: Results for noisy grid navigation task with no terminal states. Accuracy and average error for bounds based on feature counts (WFCB) compared with 99, 95, and 90 percentiles for the VaR bound. Accuracy and averages are computed over 200 replicates

6.2 Infinite horizon grid navigation

Our first task is an infinite horizon grid world navigation task with no terminal states (results for grid worlds with terminal states are similar and are reported in Appendix C). To evaluate different bounding methods we generated 200 random 9x9 worlds with random features each grid cell. For each world we generated a random feature weight vector w from the L1-unit ball using the method described in Appendix A. To generate the demonstrations we solve the MDP using the generated ground truth reward to find the optimal policy. We give trajectories of length 100 for each demonstration. We set the evaluation policy to be the optimal policy under the MAP reward function found using BIRL. Because the demonstrations are perfect, we set the BIRL confidence parameter to a large value ($c = 100$). While not the focus of our current work, in the future we believe c could also be automatically set from the demonstrations [22].

Figure 1(a) shows the accuracy of each bound where WFCB is the worst-case feature count bound, and VaR X is the $X/100$ quantile Value at Risk bound. The accuracy is calculated by counting the number of times the proposed upper bound is above the ground truth expected value difference divided by the total number of feasible rewards that were tested. Over 200 trials, the WFCB always gives an upper bound on the true performance difference between the optimal policy and the evaluation policy. The bounds on α -VaR are also highly accurate.

Because always predicting a high upper bound will result in high accuracy, we also measured the tightness of the the upper bounds. Figure 1(b) shows the average bound error over the 200 random navigation tasks. We measure the bound error as the difference between the upper bound and the ground truth EVD so the error for a bound b is given as

$$\text{error}(b) = b - \text{EVD}(\pi_{\text{eval}}, R^*) \quad (10)$$

where R^* is the generated ground truth reward. We see that the bounds on the α -VaR are much tighter than the worst-case feature count bound, converging after only a small number of demonstrations.

6.3 Noisy demonstrations

As mentioned in Section 2, BIRL uses a confidence parameter, c , that represents the optimality of the demonstrations. When $c = 0$, the demonstrations are assumed to come from a completely random policy, and $c = \infty$ means that the demonstrations come from a perfectly optimal policy. Prior work used values of c between 25 and 500 when demonstrations are generated from an expert policy [13, 14]. To investigate the effect of c on our results we generated demonstrations where at each demonstrated state there is an 80% chance of taking an optimal action and a 20% chance of taking a random action. The resulting accuracy and bound error for several choices of c are shown in Figure 2.

Adjusting c for noisy demonstrations has a clear affect on the accuracy and bound error. The bound error (Equation 10) decreases as c increases, meaning the bounds become tighter; however, when $c = 50$ the VaR bounds often underestimate the true expected value difference between the

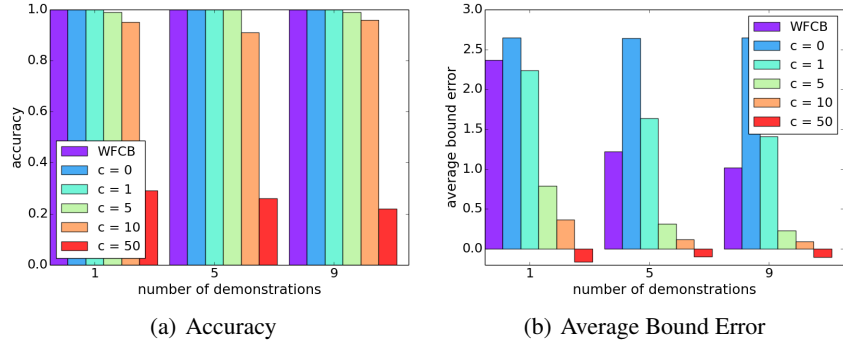


Figure 2: Sensitivity to the confidence c for noisy demonstrations in the grid navigation task. Accuracy and average error for bounds based on feature counts (WFCB) compared with 0.95-VaR bound. Accuracy and averages are computed over 200 replicates

Table 1: Comparison of bound errors for 95% confidence bound on α -VaR bound with 95% confidence Hoeffding-style bound proposed by Abbeel and Ng [1]. Both bounds use the Projection algorithm [1] to obtain the evaluation policy. All results are over 200 random navigation tasks.

Number of demonstrations	Bound Error					Average Accuracy
	1	5	9	...	15,060	
0.95-VaR Bound	0.4135	0.0896	0.0390	-	-	0.98
0.99-VaR Bound	0.6192	0.1302	0.0596	-	-	1.0
Abbeel & Ng Error Bound [1]	50.745	22.694	16.915	0.4135	-	1.0

expert’s policy and the evaluation policy, resulting in negative bound error and lower accuracy. We see that values of c in the range $(1, 10]$ result in highly accuracy bounds that are tighter than the worst-case feature count bound. However, for $c = 50$, we see that BIRL overfits to the noise in the demonstrations by assuming that the demonstrations are optimal.

6.4 Sensitivity to evaluation policy

In the previous examples we have used the MAP reward obtained from BIRL to create the evaluation policy; however, our method is applicable to any evaluation policy. We investigated the sensitivity of our bound over a range of different evaluation policies and found that the VaR bounds consistently outperforms the baseline WFCB, providing bounds that are often four times tighter in bound error while maintaining high accuracy (see Appendix D for details).

To further demonstrate the ability of our method to work with evaluation policies derived from IRL algorithms other than BIRL we used the Projection algorithm proposed by Abbeel and Ng [1] as an evaluation policy. Abbeel and Ng provide high-confidence bounds on the number of demonstrations needed for their algorithm to guarantee performance within ϵ of the demonstrator. We inverted their sample bound to obtain a $(1 - \delta)$ confidence bound on the expected value difference between the Projection algorithm and the expert’s policy given a fixed number of demonstrations (details are included in Appendix E).

We repeated the experiment described in Section 6.2 with the Projection evaluation policy. We compare the average bound error for our proposed VaR bounds with the Abbeel error bound for the Projection algorithm in Table 1. Our empirical VaR bounds are orders of magnitude tighter than the Hoeffding style bound which theoretically requires 15,060 demonstrations to match the bound error that our VaR bound achieves given only a single demonstration.

7 Related work

Many different methods exist for performing learning from demonstration through inverse reinforcement learning [2, 7]. However, few of them give any kind of sample efficient guarantees on performance. Abbeel and Ng [1] give probabilistic Hoeffding-style bounds on how many demonstrations will be required to get within epsilon of the optimal policy. However, their bounds are too loose to be useful in practice and are customized for their specific IRL algorithm. To our knowledge, we provide the first high-confidence performance bounds designed to work with any given evaluation policy.

Safety has been extensively studied within the reinforcement learning community (see Garcia et al. for a survey [8]). These approaches typically either focus on safe exploration or optimize an objective other than expected long-term reward. Recently, alternative objectives based on financial measures of risk such as VaR and Conditional VaR have been shown to provide tractable and useful risk-sensitive measures of performance for learning and planning in MDPs [18, 6]. Our work builds upon this previous work by showing how VaR can be applied to inverse reinforcement learning to enable high-confidence performance bounds.

Additional work on safety in reinforcement learning has focused on obtaining high-confidence bounds on the performance of a policy before that policy is deployed [20]. Our work draws inspiration from recent bootstrap approaches for bounding off-policy performance [19, 9]. We perform Bayesian sampling from the posterior distribution over reward functions given the demonstrations. Similar to bootstrapping, this allows us to bound an evaluation policy’s performance over many different reward functions that are likely given the demonstrations. Unlike previous work on off-policy evaluation, we provide bounds on performance loss that are applicable when learning from demonstrations, i.e., when the rewards are not observed.

8 Conclusions and future work

In this work we have formalized and addressed the problem of high-confidence policy evaluation, when the reward function is unknown. To our knowledge, we present the first general method for obtaining high-confidence bounds on the performance difference between any evaluation policy and the optimal policy for a demonstrator’s true unknown reward. One major benefit of our approach is that it makes no assumptions on the evaluation policy, thus the evaluation policy could be hand-crafted, learned from demonstrations, learned through reinforcement learning, or any combination. Thus, we believe our work is an important step towards evaluating the safety of a policy learned through demonstration, selecting between multiple candidate policies, and knowing when an agent has received enough demonstrations to learn a task.

While limited to a grid world navigation task, our empirical results that our proposed bound is a significant improvement over a baseline based on feature counts, and that it provides accurate, tight bounds even for small numbers of noisy demonstrations. Because our bound is based on Bayesian IRL, our method is designed to work with partial demonstrations and allows insertion of domain knowledge as a prior over reward functions. We believe that these attributes make our bound an ideal starting point for developing confidence bounds that are useful for real world learning from demonstration tasks.

One of the main drawbacks of our proposed VaR bound is that it requires solving an MDP at every step. Future work should investigate whether IRL methods based on policy gradients [16, 10] or other IRL algorithms that do not require repeatedly solving an MDP can be used to sample from the reward posterior. Another potential drawback of our method is that it requires knowing the initial state distribution of the demonstrator; however, this distribution could be inferred from demonstrations using a state-space similarity metric [14]. While not required, our method also benefits from knowing the transition dynamics of the MDP. Thus, investigating how model-free and model-based reinforcement learning algorithms can be inserted into our framework is another area of future work. Finally, our method relies on an appropriate confidence parameter c , which determines how much we trust the demonstrations. Recent work has used EM to learn this parameter from a large number of demonstrations from policies with varying amounts of noise [22]. Future work should investigate whether a similar approach works for a small number of demonstrations from a single demonstrator.

Appendices

A Uniform sampling from L1-unit ball

We derive an algorithm that correctly samples uniformly from the L1-norm unit ball. Our method is a special case of the result by Barthe et al. [3] as detailed in Weisstein [21]. The general result states that if we wish to sample an element from the L-p ball in d-dimensional space, then we should pick X_1, \dots, X_d independently from the pdf

$$P_p(x) = \frac{\exp(-|x|^p)}{2\Gamma(1 + p^{-1})} \quad (11)$$

where p is the desired p -norm and Γ is the gamma function. Then we draw Y from an exponential distribution with mean 1 and our resulting sample from the L_p norm ball is

$$\frac{(X_1, \dots, X_n)}{(Y + \sum_{i=1}^n |X_i|^p)^{1/p}} \quad (12)$$

We wish to sample from the L1-norm boundary, i.e. where the L1-norm is equal to 1. Thus we have $p = 1$ and $Y = 0$ above. This means that we need to sample d numbers independently from the following pdf

$$P_1(x) = \frac{\exp(-|x|)}{2\Gamma(2)} = \frac{\exp(-|x|)}{2}. \quad (13)$$

We can sample from this distribution using the inverse CDF sampling method (c.f. Bishop [4]). To draw samples from this distribution we must compute the inverse of the indefinite integral

$$z = h(x) = \int_{-\infty}^x \frac{\exp(-|\hat{x}|)}{2} d\hat{x} \quad (14)$$

Note that the desired distribution, $P_1(x)$, is a peaked distribution centered at zero, so half of the probability mass will be less than zero and half will be greater than zero. We can thus break-up our inverse of the CDF into two cases.

Case 1: If our random uniform sample $z \in [0, 1/2]$, then our resulting x should be non-positive. In this case we can write $P_1(x)$ as

$$P_1^-(x) = \frac{\exp(x)}{2} \quad (15)$$

We can now easily solve for $f(z) = h^{-1}(z)$ where

$$z = h(x) = \frac{1}{2} \int_{-\infty}^x \exp(\hat{x}) d\hat{x}. \quad (16)$$

Solving the integral and inverting gives

$$x = \ln(2z). \quad (17)$$

Case 2: $z \in [1/2, 1]$. In this case, x , our resulting sample from $P_1(x)$ should be non-negative. Thus, we can write $P_1(x)$ as

$$P_1^+(x) = \frac{\exp(-x)}{2} \quad (18)$$

We can now solve for $f(z) = h^{-1}(z)$ where this time

$$z = h(x) = \frac{1}{2} \int_{-\infty}^x \exp(-\hat{x}) \quad (19)$$

$$= \frac{1}{2} + \frac{1}{2} \int_0^x \exp(-\hat{x}) d\hat{x}. \quad (20)$$

Solving the and inverting gives

$$x = -\ln(2 - 2z). \quad (21)$$

In summary, to sample from $P_1(x) = \frac{\exp(-|x|)}{2}$ we first draw $z \sim [0, 1]$. Then we return

$$x = \begin{cases} \ln(2z), & \text{for } z < 1/2 \\ -\ln(2-2z), & \text{otherwise} \end{cases} \quad (22)$$

Using d samples from $P_1(x)$ and then normalize the resulting sample gives us a way to uniformly sample the L1-norm unit sphere. This method summarized in Algorithm 2 for uniformly sampling from the L1 unit sphere.

Algorithm 2 L1-Norm Unit Ball Sampling in \mathbb{R}^d

```

1: input:  $d$  ▷ number of dimensions
2: for  $i = 1 : d$  do
3:    $z \sim U(0, 1)$ 
4:   if  $z \leq 0.5$  then
5:      $X_i = \ln(2z)$ 
6:   else
7:      $X_i = -\ln(2 - 2z)$ 
8:  $\mathbf{X} \leftarrow (X_1, \dots, X_d) / \sum_{i=1}^d |X_i|$ 
9: return  $\mathbf{X}$ 

```

Our MCMC implementation of BIRL ensures that each proposal step remains on the L1-norm unit ball. We use Algorithm 3 to generate a proposal by taking a small step along each pair of axis while staying on the L1-norm unit ball. For each pair of axis we use Algorithm 4 to step along the manifold defined by the two axis.

B Implementation and simulation details

In all of our grid world experiments we use $\text{stepSize} = 0.01$ for the L1-Norm Unit Ball Walk described in Algorithm 3. We run MCMC for 10000 steps using a burn-in of 100 samples and only using every 20th sample to avoid autocorrelation effects.

We found that the BIRL likelihood can be sensitive to data imbalance if the demonstrations contain some state-action pairs much more frequently than others. To ameliorate this problem, we remove duplicate state-action pairs for infinite horizon problems.

Examples of a randomly generated grid navigation world with a single terminal goal state (blue) and a randomly generated infinite horizon grid navigation world are shown in Figure 3. We use $\gamma = 0.95$ for the navigate task with a terminal goal and $\gamma = 0.9$ for the infinite horizon navigation task.

C Experiments for navigate-to-goal grid world

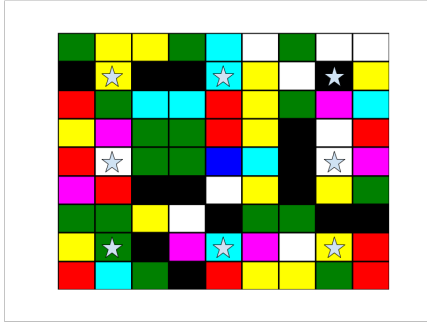
C.1 Grid world with terminal goal state

We also ran experiments using a single terminal goal state. To evaluate different bounding methods we generated 200 random 9x9 worlds with a unique terminal goal state in the center and random features for all other grid cells. For each random world we generated a random feature weight vector w such that $\|w\|_1 = 1$ such that the feature weight associated with the terminal is non-negative and that all other weights are non-positive. This ensures that most randomly generated reward functions are such that all optimal trajectories from the initial states reach the goal state. If this is not the case, then we repeatedly resample random reward functions using Algorithm 2 (with appropriate sign changes) until this is true. This allows us to evaluate the bounds over a wide range of possible ground truth rewards that explain the same navigate-to-goal behavior without biasing our results by fixing a single ground truth reward or feature configuration. We examine the affects of both optimal and sub-optimal demonstrations, as well as the sensitivity of our approach to the confidence parameter c and choice of evaluation policy, π_{eval} .

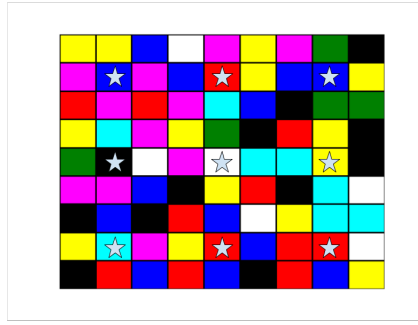
We set the evaluation policy to be the optimal policy under the MAP reward function found using BIRL. To generate the demonstrations we solve the MDP to find the optimal policy. Because the

Algorithm 3 L1-Norm Unit Ball Walk

```
1: input:  $w \in \mathbb{R}^d$ , stepSize ▷ initial weight vector
2: for each pair of dimensions  $(i, j) : i, j = 1, \dots, d$  do
3:   direction  $\leftarrow$  random('clockwise', 'counterclockwise')
4:   if  $w[i]$  is not 0 or  $w[j]$  is not 0 then
5:      $w[i], w[j] \leftarrow$  L1ManifoldStep( $w[i], w[j],$  direction,  $\eta$ )
6: return  $w$ 
```



(a) Grid world with terminal goal state at center



(b) Grid world with no terminal states

Figure 3: Random grid world navigation tasks. Stars denote initial states from which demonstrations are given. (a) Blue is the goal terminal state. All features have non-positive random weights except for blue which has non-negative weight. (b) There are no terminal states and features have random weights.

demonstrations are perfect, we set the BIRL confidence parameter to a large value ($c = 100$). Figure 4 shows the resulting accuracy and bound error as the number of demonstrations is increased. We see that, over 200 trials, the WFCB always gives an upper bound on the true performance difference between the optimal policy and the evaluation policy. We see that the different percentile bounds are also highly accurate. We also see that all of the VaR percentile bounds are much tighter than the worst-case bound, especially for small numbers of demonstrations. As the number of demonstrations increases the error for all the bounds tends towards zero.

C.2 Sensitivity to confidence parameter for optimal demonstrations

To test whether the above results are sensitive to the confidence parameter c we repeated the above navigate-to-goal experiment for several values of c . The results are shown in Figure 5 Using smaller values of c increase the bound error as MCMC will accept a wider range of rewards, many of which have optimal policies very different from the evaluation policy. Despite the sensitivity, we see that for $c > 10$ we achieve high accuracy and low bound errors. This motivates our use of $c = 100$ in experiments involving optimal demonstrations.

D Sensitivity to evaluation policy

In the previous examples we have used the MAP reward obtained from BIRL to create the evaluation policy; however, our method is applicable to any evaluation policy. We also investigate how the accuracy and bound error obtained from our VaR bound is affected by the choice of evaluation policy we ran an experiment where we varied the optimality of the evaluation policy. As before, we generated 200 random rewards for evaluation. The evaluation policy was chosen by taking the optimal policy obtained from the ground truth reward and selecting X states at random without replacement and changing the policy at those X states so that it takes a non-optimal action. All demonstrations were optimal so we computed the VaR bounds using $c = 100$.

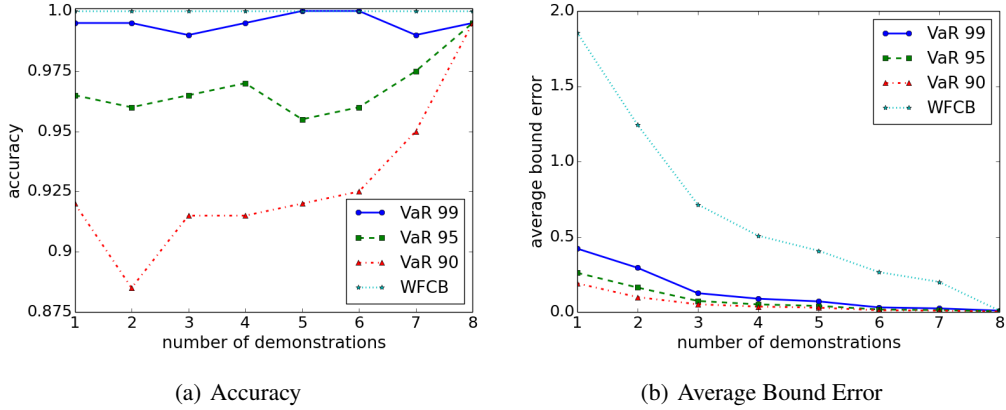


Figure 4: Results for grid navigate-to-goal task. Accuracy and average error for bounds based on feature counts (WFCB) compared with 99, 95, and 90 percentiles for the VaR bound. Accuracy and averages are computed over 200 replicates.

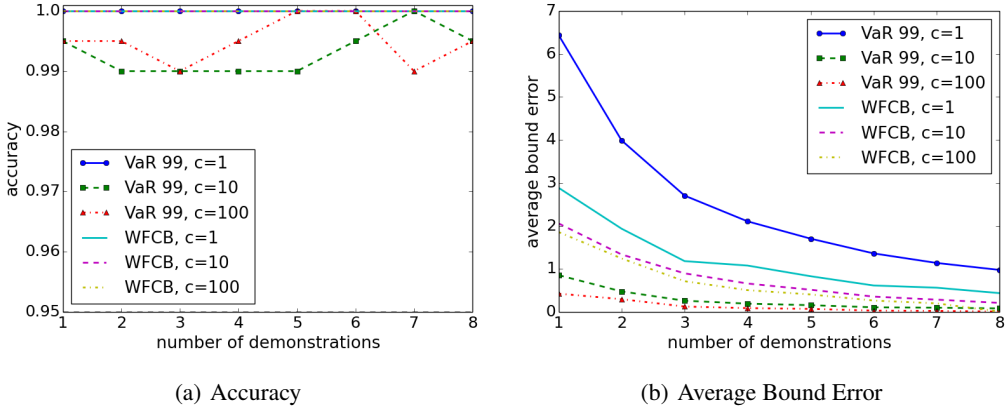


Figure 5: Effects of varying BIRL confidence parameter c on the navigate-to-goal task. Accuracy and average error for bounds based on feature counts (WFCB) compared with $\alpha = 0.99$ for the VaR bound.

The results for $X = 0, 2, 4, 8, 16, 32, 64$ after one demonstration and after nine demonstrations are shown in Figure 6. When the evaluation matches the optimal policy under the true reward ($X = 0$) all bound methods always gave true upper bounds on the EVD. When only one demonstration is given, there is a large bound error for all methods, with WFCB giving an error bound 4 times higher than the worst VaR bound error. As X is increased, the evaluation policy becomes more dissimilar to the optimal policy the accuracy of all methods, except for the extremely cautious 0.99-VaR decreases. When 9 demonstrations are given, the VaR bounds are much tighter with almost zero error for evaluation bounds close to optimal. The accuracy tends to drop as the number of errors increases, but still remains above 95% even for a policy that differs from the optimal policy in over 75% of the states.

E Using projection algorithm to obtain evaluation policy

Abbeel and Ng [1] give sample efficiency bounds for the number of demonstrations required to get within ϵ of an experts performance. We summarize their result as the following theorem.

Theorem 1. *To obtain a policy $\hat{\pi}$ such that with probability $(1 - \delta)$*

$$\epsilon \geq |V^{\hat{\pi}}(R^*) - V^{\pi^*}(R^*)| \quad (23)$$

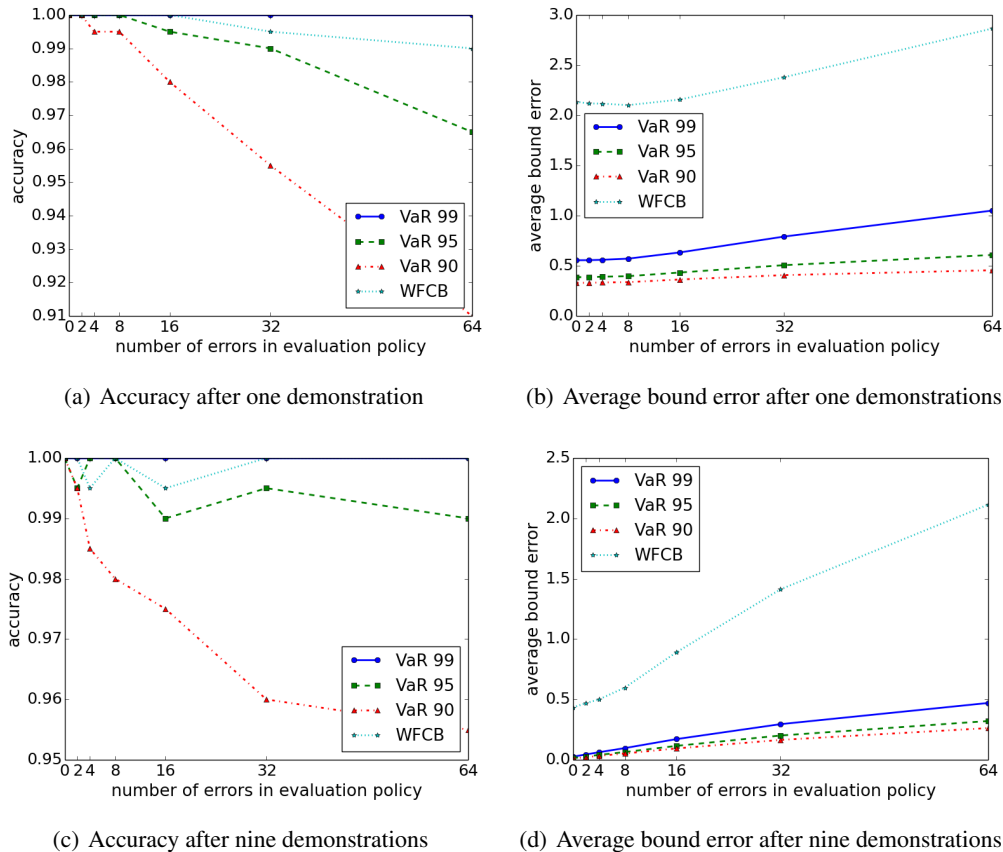


Figure 6: Sensitivity over range of evaluation policies. Results are averaged over 200 grid navigation task with no terminal states. Accuracy and average error for bounds based on feature counts (WFCB) compared with 99, 95, and 90 percentiles for the VaR bound.

it suffices to have

$$m \geq \frac{2k}{(\epsilon(1-\gamma))^2} \log \frac{2k}{\delta}. \quad (24)$$

Often we are simply given a fixed set of demonstrations and wish to know how far from optimal performance our learn policy is. Using the same proof technique as Abbeel and Ng [1] we obtained the following corollary for a fixed number of demonstrations and a desired confidence level, δ .

Corollary 1. *Given a confidence level δ , and m demonstrations, with probability $(1 - \delta)$ we have that $|V^{\pi^*}(R^*) - V^{\hat{\pi}}(R^*)| \leq \epsilon$, where*

$$\epsilon = \frac{2\sqrt{k}}{1-\gamma} \sqrt{\frac{-1}{2m} \log \frac{\delta}{2k}} \quad (25)$$

where k is the number of features and γ is the discount factor of the underlying MDP.

References

- [1] Pieter Abbeel and Andrew Y Ng. Apprenticeship learning via inverse reinforcement learning. In *Proceedings of the twenty-first international conference on Machine learning*, page 1. ACM, 2004.
- [2] Brenna D. Argall, Sonia Chernova, Manuela Veloso, and Brett Browning. A survey of robot learning from demonstration. *Robotics and Autonomous Systems*, 57(5):469–483, 2009.
- [3] Franck Barthe, Olivier Guédon, Shahar Mendelson, Assaf Naor, et al. A probabilistic approach to the geometry of the ℓ_p^n -ball. *The Annals of Probability*, 33(2):480–513, 2005.

- [4] Christopher M Bishop. *Pattern recognition and machine learning*. springer, 2006.
- [5] Jaedeug Choi and Kee-Eung Kim. Map inference for bayesian inverse reinforcement learning. In *Advances in Neural Information Processing Systems*, pages 1989–1997, 2011.
- [6] Yinlam Chow, Aviv Tamar, Shie Mannor, and Marco Pavone. Risk-sensitive and robust decision-making: a cvar optimization approach. In *Advances in Neural Information Processing Systems*, pages 1522–1530, 2015.
- [7] Yang Gao, Jan Peters, Antonios Tsourdos, Shao Zhifei, and Er Meng Joo. A survey of inverse reinforcement learning techniques. *International Journal of Intelligent Computing and Cybernetics*, 5(3):293–311, 2012.
- [8] Javier Garcia and Fernando Fernández. A comprehensive survey on safe reinforcement learning. *Journal of Machine Learning Research*, 16(1):1437–1480, 2015.
- [9] Josiah P Hanna, Peter Stone, and Scott Niekum. High confidence off-policy evaluation with models. *arXiv preprint arXiv:1606.06126*, 2016.
- [10] Jonathan Ho, Jayesh Gupta, and Stefano Ermon. Model-free imitation learning with policy optimization. In *International Conference on Machine Learning*, pages 2760–2769, 2016.
- [11] Myles Hollander and Douglas A Wolfe. *Nonparametric Statistical Methods: By Myles Hollander, Douglas A. Wolfe*. J. Wiley, 1999.
- [12] Philippe Jorion. *Value at risk*. McGraw-Hill, New York, 1997.
- [13] Manuel Lopes, Francisco Melo, and Luis Montesano. Active learning for reward estimation in inverse reinforcement learning. In *Joint European Conference on Machine Learning and Knowledge Discovery in Databases*, pages 31–46. Springer, 2009.
- [14] Bernard Michini and Jonathan P How. Improving the efficiency of bayesian inverse reinforcement learning. In *Robotics and Automation (ICRA), 2012 IEEE International Conference on*, pages 3651–3656. IEEE, 2012.
- [15] Andrew Y Ng, Stuart J Russell, et al. Algorithms for inverse reinforcement learning. In *Icml*, pages 663–670, 2000.
- [16] Matteo Pirota and Marcello Restelli. Inverse reinforcement learning through policy gradient minimization. In *AAAI*, pages 1993–1999, 2016.
- [17] Deepak Ramachandran and Eyal Amir. Bayesian inverse reinforcement learning. *Urbana*, 51(61801):1–4, 2007.
- [18] Aviv Tamar, Yonatan Glassner, and Shie Mannor. Optimizing the cvar via sampling. In *Proceedings of the Twenty-Ninth AAAI Conference on Artificial Intelligence*, pages 2993–2999. AAAI Press, 2015.
- [19] Philip Thomas, Georgios Theodorou, and Mohammad Ghavamzadeh. High confidence policy improvement. In *Proceedings of the 32nd International Conference on Machine Learning (ICML-15)*, pages 2380–2388, 2015.
- [20] Philip S Thomas, Georgios Theodorou, and Mohammad Ghavamzadeh. High-confidence off-policy evaluation. In *AAAI*, pages 3000–3006, 2015.
- [21] EW Weisstein. Ball point picking. *From MathWorld—A Wolfram Web Resource*. <http://mathworld.wolfram.com/BallPointPicking.html>, 2017.
- [22] Jiangchuan Zheng, Siyuan Liu, and Lionel M Ni. Robust bayesian inverse reinforcement learning with sparse behavior noise. In *AAAI*, pages 2198–2205, 2014.
- [23] Brian D Ziebart, Andrew L Maas, J Andrew Bagnell, and Anind K Dey. Maximum entropy inverse reinforcement learning. In *AAAI*, pages 1433–1438, 2008.

Algorithm 4 L1ManifoldStep

```
1: input:  $w1, w2 \in \mathbb{R}$ , direction, stepSize
2: slack =  $w1 + w2$ 
3: clockwisePos = ["+", "-", "- ", "- +"]
4: clockwiseDir = [+1, -1, +1, -1]
5: counterclockwisePos = ["+ +", "- +", "- -", "+ -"]
6: counterclockwiseDir = [-1, +1, -1, +1]
7: sign1 = ( $w1 \geq 0$ )
8: sign2 = ( $w2 \geq 0$ ) ▷ find starting quadrant
9: if sign1 and sign2 then
10:   cyclePos = "+ +"
11: else if sign1 and not sign2 then
12:   cyclePos = "+ -";
13: else if not sign1 and sign2 then
14:   cyclePos = "- +"
15: else
16:   cyclePos = "- -"
17: if direction is "clockwise" then ▷ find direction to change magnitude of w1
18:   cycleIndx = clockwisePos.indexOf(cyclePos)
19: else
20:   cycleIndx = counterclockwisePos.indexOf(cyclePos)
21: stepRemaining = stepSize
22: while stepRemaining > 0 do ▷ step along 1-D manifold of L1-unit ball in 2-D
23:   if direction is "clockwise" then
24:     cycleDir = clockwiseDir[cycleIndx]
25:   else
26:     cycleDir = counterclockwiseDir[cycleIndx]
27:   maxStep = stepRemaining
28:   if (cycleDir is 1) and (( $|w1| + cycleDir * stepRemaining$ ) > slack) then
29:     maxStep = slack -  $|w1|$ 
30:     cycleIndx = mod(cycleIndx + 1, 4)
31:   else if (cycleDir is -1) and (( $|w1| + cycleDir * stepRemaining$ ) < 0) then
32:     maxStep =  $|w1|$ 
33:     cycleIndx = mod(cycleIndx + 1, 4)
34:    $w1 = |w1| + cycleDir * maxStep$ 
35:    $w2 = |w2| - cycleDir * maxStep$ 
36:   stepRemaining = stepRemaining - maxStep
37:   if randDir is "clockwise" then ▷ determine correct signs based on final quadrant
38:     cyclePos = clockwisePos[cycleIndx]
39:   else
40:     cyclePos = counterclockwisePos[cycleIndx]
41:   if cyclePos is "- +" then
42:      $w1 = -w1$ 
43:   else if cyclePos is "+ -" then
44:      $w2 = -w2$ 
45:   else if cyclePos is "- -" then
46:      $w1 = -w1$ 
47:      $w2 = -w2$ 
48: return  $w1, w2$ 
```
